Subband structure of n-channel inversion layers on polar semiconductors

G. H. Kawamoto, J. J. Quinn, and W. L. Bloss

Brown University, Providence, Rhode Island 02912

(Received 22 August 1980)

The subband structure of n-channel inversion layers on the surface of polar semiconductors has been investigated. The model used includes the effects of the Coulomb interaction and the polar, LO-phonon-mediated electron-electron interaction. The Coulomb interaction has been treated in the so-called diagonal random-phase approximation. This approximation ignores the effects of subband mixing, but is known to be valid for Coulomb forces. However, the phonon interaction is frequency dependent and may strongly mix states in different subbands, particularly when subband separation is near ω_{LO}, the LO-phonon frequency. Therefore, the calculation includes the effects of subband mixing due to an unscreened electron–LO-phonon interaction. A simple two-subband model has been used to calculate the quasiparticle energies and subband separation as a function of wave vector and density. In addition, the effect of the electron-phonon interaction on the depolarization shift has been investigated. It is found that the frequency dependence of this interaction splits each absorption peak into two branches which can be interpreted as mixed intersubband–LO-phonon excitations. The magnitude of the splitting and the relative strength of each absorption peak has been calculated.

INTRODUCTION

In an earlier calculation,[1] we discussed the subband structure of n-channel inversion layers on the surface of polar semiconductors and, in particular, on the surface of GaAs. That calculation included the many-particle effects of the electron-electron interaction which, on polar semiconductors, is the sum of a Coulomb repulsion and a term due to the exchange of virtual longitudinal-optical (LO) phonons. The latter effect is not present in the elemental (nonpolar) semiconductors, silicon and germanium. The calculation was performed using the diagonal random-phase approximation (RPA) (Ref. 2) and, therefore, ignored the effects of intersubband mixing.

In this paper, we extend our previous calculation by partially removing the restrictions of the diagonal approximation. The method includes the effects of intersubband mixing due to an *unscreened* phonon-mediated interaction, but continues to treat the Coulomb interaction using the diagonal RPA. Using this model, we have calculated the self-energies and quasiparticle energies of electrons in the two lowest subbands of n-channel inversion layers on polar semiconductors. The calculation has been performed at zero temperature assuming that only the ground subband is occupied. A simple two-subband model has been used to truncate the Green's-function matrix. The results presented are correct for inversion layers on p-type GaAs (assuming a native oxide insulator) and p-type InP (assuming a deposited SiO_2 insulator).

In addition, we have calculated the subband separation and the depolarization shift[3] which would be observed in a far-infrared (FIR) absorption experiment. The depolarization calculation includes the effects of a frequency-dependent interaction (the phonon contribution to the total electron-electron interaction), and indicates that, in polar semiconductors, each absorption peak normally associated with an intersubband transition is split into two branches which are interpreted as mixed electron-phonon excitations. (This splitting, however, does not explain the "double" peak observed in InSb inversion layers.[4]) The absorption energy and relative strength of each peak have been calculated as a function of inversion-layer density.

The basis of the calculation is the solution of the effective-mass Hartree equation discussed briefly in the next section. In Sec. II the electron-electron interaction is discussed and an explicit form for the phonon-mediated contribution is derived from the Fröhlich Hamiltonian. In Sec. III we discuss the methods used in the many-particle calculation of the self-energy and present the results of the present calculation. Finally the depolarization effect and results are described in Sec. IV.

I. HARTREE SOLUTION

Within the effective-mass approximation,[5] the Hartree wave function, $\psi_{i,\vec{k}}(\vec{x})$, satisfies a Schrödinger-type equation of the form

$$\left(-\frac{\hbar^2}{2m^*}\nabla^2 + V(z)\right)\psi_{i,\vec{k}}(x) = \epsilon_i(\vec{k})\psi_{i,\vec{k}}(x). \tag{1}$$

The eigenvalue, $\epsilon_i(\vec{k})$, is the particle energy and has been calculated here within the Hartree approximation. The conduction band of GaAs and InP (as well as many other III-V semiconductors) contains a single (nondegenerate), isotropic valley at the Brillouin-zone center. Therefore the band effective mass, m^*, appearing in Eq. (1) is a

scalar quantity that is independent of the interface plane.

The confining potential, $V(z)$, is the sum of the depletion layer potential and the self-consistent Hartree potential which has been calculated assuming that only the ground subband is occupied at $T = 0$ K. Since the potential is independent of the coordinates x and y (which define the interface plane), the Schrödinger equation is separable. That is, $\psi_{i,\vec{k}}$ can be written as the product of a plane-wave part $(e^{i\vec{k}\cdot\vec{r}})$ and a bound part $[\xi_i(z)]$:

$$\psi_{i,\vec{k}}(x) = \frac{1}{\sqrt{A}} e^{i\vec{k}\cdot\vec{r}} \xi_i(z), \qquad (2)$$

where $\xi_i(z)$ satisfies the one-dimensional equation

$$\left(-\frac{\hbar^2}{2m^*}\frac{d^2}{dz^2} + V(z)\right)\xi_i(z) = E_i\xi_i(z). \qquad (3)$$

The energy eigenvalues, E_i, and the Hartree wave functions, ξ_i, have, in the past, been found using a number of different approximate methods including the direct numerical solution of Eq. (3). We have adopted a variational approach[6] which has been used successfully in the many-particle description of inversion layers on the surface of silicon. Here, the wave function is approximated by

$$\xi_i(z) = \sum_{j=0}^{i} g_{ij} z^{j+1} e^{-p_i z}, \quad i = 0, 1, 2, \ldots. \qquad (4)$$

The g_{ij} are determined (as functions of p_i) by requiring that the ξ_i are normalized and orthogonal to each other. The p_i can then be adjusted until E_i is a minimum.

II. THE ELECTRON-ELECTRON INTERACTION

The total electron-electron interaction, V^{e-e}, may be written as the sum of a Coulomb term, V^{Coul}, and a contribution arising from the exchange of a virtual LO phonon, V^{e-ph}. Since the total interaction and its individual components are usually assumed to be translationally invariant in the plane of the interface (but not necessarily perpendicular to the interface) and in time, they may be described by their transforms with respect to the Hartree wave functions, $\psi_{i,\vec{k}}$. Thus,

$$V^{e-e}_{ijlm}(\vec{q}, \omega) = V^{Coul}_{ijlm}(\vec{q}) + V^{e-ph}_{ijlm}(\vec{q}, \omega). \qquad (5)$$

This quantity has physical interpretation as the strength of the interaction which takes the state $\psi_{i,\vec{k}}$ to $\psi_{j,\vec{k}-\vec{q}}$, transfers momentum $\hbar\vec{q}$ and energy $\hbar\omega$ and takes the state $\psi_{l,\vec{k}}$ to $\psi_{m,\vec{k}+\vec{q}}$.

The Coulomb portion of the interaction is well known from studies on silicon inversion layers.[7]

It is usually expressed as the sum of a direct contribution and an image contribution

$$V^{Coul}_{ijlm}(\vec{q}) = V^{dir}_{ijlm}(\vec{q}) + V^{im}_{ijlm}(\vec{q}), \qquad (6)$$

where

$$V^{dir}_{ijlm}(\vec{q}) = \left(\frac{1}{A}\right)\left(\frac{2\pi e^2}{\epsilon_\infty q}\right)$$

$$\times \int_0^\infty dz \int_0^\infty dz' \xi_i(z)\xi_j^*(z)$$

$$\times e^{-q|z-z'|}\xi_l^*(z')\xi_m(z'), \qquad (7)$$

and

$$V^{im}_{ijlm}(q) = \left(\frac{1}{A}\right)\left(\frac{2\pi e^2}{\epsilon_\infty q}\right)\left(\frac{\epsilon_\infty - \epsilon_i}{\epsilon_\infty + \epsilon_i}\right)$$

$$\times \int_0^\infty dz \int_0^\infty dz' \xi_i(z)\xi_j^*(z)$$

$$\times e^{-q(z+z')}\xi_l^*(z')\xi_m(z'). \qquad (8)$$

Here ϵ_∞ is the high-frequency dielectric constant of the semiconductor and ϵ_i is the insulator dielectric constant. The direct term, V^{dir}_{ijlm}, represents the interaction strength of the Coulomb repulsion between two electrons imbedded in a medium with dielectric constant ϵ_∞. The image term, V^{im}_{ijlm}, describes an additional Coulomb interaction between an inversion-layer electron and the *image* of *another* electron in the insulating layer.

Within the framework of a many-particle calculation, the electron-phonon interaction manifests itself as an *effective interaction between electrons*. As mentioned, the interaction may be interpreted as arising from the exchange of a virtual phonon. More physically, it can be understood by noting that an electron (or other charged particle) moving through a polarizable crystal (i.e., a crystal composed of ions with different charge) will polarize the lattice. Other electrons can then interact with the first *indirectly* via the polarized lattice. The polar interaction is *not* present in the elemental semiconductors (silicon and germanium) because the lattice is not polarizable.

In diamond structure (silicon or germanium) or zinc-blende structure (GaAs, InSb, InP, etc.) semiconductors, symmetry requires the existence of six different phonon modes (though there are additional degeneracies in the diamond structure). In particular, there are three acoustic modes and three optical modes each with two transverse branches (TA and TO) and one longitudinal (LA and LO) branch. While electrons are coupled to all six modes, it can be rigorously demonstrated[8] that the coupling to transverse modes is negligible compared to the coupling with longitudinal modes.

The present calculation includes coupling only

with LO-phonon modes. The neglect of the LA modes can be partially justified by noting that the ionic displacement of oppositely charged ions due to acoustic vibrations tends, particularly at the long wavelengths of interest, to be in the same direction. The lattice polarization results only because the oppositely charged ions have different masses and are not displaced by the same amount. Therefore the resulting polarization can be rather small, particularly in semiconductors like GaAs or InSb where the ionic masses differ by less than 10%. In contrast, oppositely charged ions are displaced in opposite directions by long-wavelength LO excitations. The polarization field and its coupling to electrons might, therefore, be expected to be stronger for LO modes than for LA modes.

In the following, the coupling between inversion-layer electrons and _bulk_ LO phonons is described, and an explicit form for the effective, phonon-mediated, electron-electron interaction is derived. The treatment loosely follows those of Refs. 8 and 9, but the derivation here is in the context of the inversion-layer problem. The interaction is obtained in two steps. First, a Fröhlich Hamiltonian valid for a quasi-two-dimensional (2D) system (but with coupling to bulk phonons) is derived. The result is then used in a second-order Born approximation to obtain the actual interaction strength.

It is convenient to begin with a form of the Fröhlich Hamiltonian which is properly second quantized in the phonons but not the electrons[9] as follows:

$$H^{e\text{-ph}}_{(r,z)} = \frac{1}{\sqrt{V}} \sum_{\vec{q},\,q_z} M^{ph}_{(\vec{q},\,q_z)} [\hat{a}(\vec{q},q_z) + \hat{a}^\dagger(-\vec{q},-q_z)] e^{i\vec{q}\cdot\vec{r}_e} e^{iq_z z},$$

(9)

where $\hat{a}^\dagger$ and $\hat{a}$ are, respectively, the phonon creation and destruction operators, and

$$M^{ph}_{(\vec{q},\,q_z)} = (i)\left[\frac{2\pi e^2}{(q^2+q_z^2)}(\hbar\omega_{LO})\left(\frac{1}{\epsilon_\infty}-\frac{1}{\epsilon_0}\right)\right]^{1/2}. \quad (10)$$

Notice that the LO phonons have been assumed dispersionless (their frequency is independent of $\vec{q}$). The Hamiltonian, fully second quantized in both the phonons and electrons, may be found immediately from Eq. (9) as

$$\hat{H}^{e\text{-ph}} = \sum_{i,\,j;\,\vec{k},\,\vec{k}} \langle(j,\vec{k}')|H^{e\text{-ph}}_{(\vec{q},z)}|(i,\vec{k})\rangle \hat{c}^\dagger_{(j,\vec{k})}\hat{c}_{(i,\vec{k})},$$

(11)

where $\hat{c}^\dagger_{(i,\vec{k})}$ and $\hat{c}_{(i,\vec{k})}$ are creation and destruction operators for the electronic state $\psi_{i,\vec{k}}$. Conservation of momentum in the plane parallel to the interface requires that $\vec{k}' = \vec{k}+\vec{q}$. Thus

$$H^{e\text{-ph}} = \frac{1}{\sqrt{V}} \sum_{i,\,j;\,\vec{k},\,\vec{q}} \sum_{q_z} M^{ph}_{ij}(\vec{q},q_z)[\hat{a}(\vec{q},q_z)+\hat{a}^\dagger(-q,-q_z)]$$

$$\times \hat{c}^\dagger(j,\vec{k}+\vec{q})\hat{c}(i,\vec{k}), \quad (12)$$

where

$$M^{ph}_{ij}(\vec{q},q_z) = M^{ph}(\vec{q},q_z)\int_0^\infty dz\,\xi_j^*(z)\,\xi_i(z)e^{iq_z z}. \quad (13)$$

The result, Eq. (12), is similar to the three-dimensional form for the Fröhlich Hamiltonian. The principal difference is an additional sum over q_z which arises because momentum is not conserved perpendicular to the interface. In effect q_z need not be specified in a collision and, therefore, the Hamiltonian is, properly, an average over all possible values of this quantity.

The effective interaction resulting from the exchange of a virtual LO phonon may be found by applying the second Born approximation[8] to Eq. (12):

$$V^{e\text{-ph}}_{ijlm(\vec{q},\omega)} = \sum_I \frac{\langle(j,\vec{k}-\vec{q})(m,\vec{k}'+\vec{q})|H^{e\text{-ph}}|I\rangle\langle I|H^{e\text{-ph}}|(i,\vec{k})(l,\vec{k}')\rangle}{[\epsilon_i(\vec{k})+\epsilon_l(\vec{k}')]-\epsilon_I}. \quad (14)$$

Here $|I\rangle$ is an intermediate state whose total energy, ϵ_I, may include the energy of a virtual LO phonon. The resonance denominator is the difference between the energy of the initial or final states and the energy of the intermediate state.

The form of the Fröhlich Hamiltonian guarantees that the matrix elements vanish unless the intermediate state contains exactly one phonon more or one phonon less than the initial and final states. Then, for dispersionless phonons, a straightforward calculation yields

$$V^{e\text{-ph}}_{ijlm}(\vec{q},\omega) = \left(\frac{1}{V}\sum_{q_z} M_{ij}(\vec{q},q_z)M_{lm}(-q,-q_z)\right)\left(\frac{2\hbar\omega_{LO}}{(\hbar\omega)^2-(\hbar\omega_{LO}^2)}\right), \quad (15)$$

where

$$\hbar\omega = \epsilon_i(\vec{k})-\epsilon_j(\vec{k}-\vec{q}) = \epsilon_m(\vec{k}'+\vec{q})-\epsilon_l(\vec{k}') \quad (16)$$

is the energy transferred in the collision. The sum over q_z may be evaluated using a contour integration with the result

$$V_{ijlm}^{e\text{-ph}}(\vec{q}, \omega) = \frac{1}{A}\left(\frac{1}{\epsilon_\infty} - \frac{1}{\epsilon_0}\right)\left(\frac{2\pi e^2}{q}\right)\left(\frac{\omega_{LO}^2}{\omega^2 - \omega_{LO}^2}\right) \int_0^\infty dz \int_0^\infty dz'\, \xi_i(z)\xi_j^*(z)e^{-q|z-z'|}\xi_l(z')\xi_m(z') \qquad (17)$$

$$= \left(1 - \frac{\epsilon_\infty}{\epsilon_0}\right)V_{ijlm}^{dir}(\vec{q})\left(\frac{\omega_{LO}^2}{\omega^2 - \omega_{LO}^2}\right). \qquad (18)$$

The last form shows that the phonon-mediated interaction is proportional to a term $(1 - \epsilon_\infty/\epsilon_0)$ that is related to the polar nature of the semiconductor. Since the lattice is polarizable, $\epsilon_0 > \epsilon_\infty$ and the coupling is nonzero. Conversely, in non-polar materials, $\epsilon_0 = \epsilon_\infty$ and the phonon-mediated interaction vanishes.

Notice also that $V_{ijlm}^{e\text{-ph}}(\vec{q}, \omega)$ is frequency dependent. This dependence arises because, unlike the Coulomb force which acts (for practical purposes) instantaneously, phonon effects propagate at the speed of sound. As might be expected, the phonon term is infinite at $\omega = \pm\omega_{LO}$, the natural oscillation frequency of the lattice.

III. THE SELF-ENERGY

A. Theory

The quantity of principal interest in a many-particle calculation is the particle propagator or Green's function. In the inversion-layer problem, the transform of this function *with respect to the Hartree wave functions* $(\psi_{i,\vec{k}})$ is a matrix whose elements are labeled by the subband indices i. The quasiparticle excitation energies occur at the poles of the Green's function, or in the case of a matrix $\vec{G}$, at the values $\omega(k)$ such that

$$\det[\vec{G}^{-1}(\vec{k}, \omega(\vec{k}))] = |\vec{G}^{-1}(\vec{k}, \omega(\vec{k}))| = 0. \qquad (19)$$

A related quantity is the noninteracting Green's-function matrix, $\vec{G}^0(\vec{k}, \omega)$. This is the Green's function for a system in which there is no electron-electron interaction. Its elements have the particularly simple form

$$G_{ij}^0(\vec{k}, \omega) = \delta_{ij}G_{ii}^0(\vec{k}, \omega), \qquad (20)$$

$$G_{ij}^0(\vec{k}, \omega) = \delta_{ij}\left(\frac{\Theta(\epsilon_F - \epsilon_i(\vec{k}))}{\omega - (1/\hbar)[\epsilon_i(\vec{k}) - \epsilon_F] - i\eta}\right.$$
$$\left. + \frac{1 - \Theta(\epsilon_F - \epsilon_i(k))}{\omega - (1/\hbar)[\epsilon_i(\vec{k}) - \epsilon_F] + i\eta}\right), \qquad (21)$$

where $\epsilon_i(k)$ is the (unperturbed) Hartree energy, ϵ_F is the Fermi energy, and η is a positive infinitesimal. Notice that $\vec{G}^0(k, \omega)$ is diagonal in its subband indices indicating that the subband index is a "good" quantum number. That is, in the absence of an electron-electron interaction, there is *no* intersubband mixing.

The interacting and noninteracting Green's functions are related by Dyson's equation (a matrix equation in the inversion-layer problem) as

$$\vec{G}(\vec{k}, \omega) = \vec{G}^0(\vec{k}, \omega) + \vec{G}^0(\vec{k}, \omega)\vec{M}(\vec{k}, \omega)\vec{G}(\vec{k}, \omega) \qquad (22)$$

$$= \{[\vec{G}^0(\vec{k}, \omega)]^{-1} - \vec{M}(\vec{k}, \omega)\}^{-1}. \qquad (23)$$

$\vec{M}(\vec{k}, \omega)$ is the self-energy matrix which contains all the details of the interparticle interaction. It has been calculated here within the framework of the random phase approximation (RPA). That is, the elements of the self-energy matrix are calculated using the integral[2]

$$\hbar M_{ij}(\vec{k}, \omega) = (i)\frac{A}{(2\pi)^3}$$

$$\times \sum_l \int d^2k'\, d\omega'\, U_{illj}^{e\text{-}e}(k', \omega')$$

$$\times G_{ll}^0(k - k', \omega - \omega')e^{i\omega'\eta}, \qquad (24)$$

where $U_{ijlm}^{e\text{-}e}(\vec{k}, \omega)$ is the RPA approximation to the "dressed" electron-electron interaction.

Our earlier calculation[1] of subband structure in polar semiconductors utilized the so-called "diagonal" approximation in which the bare interaction assumed the particularly simple form

$$V_{ijlm}^{e\text{-}e}(\vec{q}) = \delta_{ij}\delta_{lm}V_{iill}^{e\text{-}e}(\vec{q}). \qquad (25)$$

A similar dependence on the subband indices was also found for the dressed interaction. But interactions of this form cannot mix states in different subbands. The subband index, therefore, remains a good quantum number and both the Green's-function matrix and the self-energy matrix are diagonal (hence the "diagonal" approximation).

It has been demonstrated by direct numerical calculation[6] that the Coulomb interaction is in fact small unless $i = j$ and $1 = m$. Thus the diagonal approximation is reasonably valid for Coulomb forces. Since the phonon-mediated interaction is proportional to the direct Coulomb term, it is reasonable to expect that $V_{ijlm}^{e\text{-ph}}$ can also be approximated by a diagonal form. However, the phonon interaction is frequency dependent and resonant at $\omega = \pm\omega_{LO}$. Thus, while the diagonal approximation is generally valid for $V_{ijlm}^{e\text{-ph}}$, subband mixing effects may become important when the subband separation is nearly equal to the LO-phonon energy.

In the present calculation, we continue using the

diagonal approximation to treat the Coulomb force. However, the intersubband mixing due to an unscreened phonon-mediated interaction is investigated by using a total dressed (Coulomb plus phonon) interaction of the form

$$U_{ijlm}^{e-e}(\vec{q}, \omega) = \delta_{ij}\delta_{lm}U_{iill}^{Coul}(\vec{q}, \omega) + V_{ijlm}^{e-ph}(\vec{q}, \omega). \quad (26)$$

As in earlier calculations on silicon inversion layers,[2] the screened Coulomb part of the interaction is found using the Dyson's equation

$$U_{iill}^{Coul} = V_{iill}^{Coul} + V_{ii00}^{Coul}\pi_{00}^{(0)}U_{00ll}^{Coul}. \quad (27)$$

This special form for U^{Coul} is valid if V_{ijlm}^{Coul} is diagonal and if only the ground subband is occupied. The latter assumption guarantees that $\pi_{nn'}^{(0)}$ is zero unless either n or n' is zero.

$\pi_{n,n'}^{(0)}$ is the lowest-order "bubble" approximation to the polarizability. In the current calculation, it (or really the total screening term $\epsilon_{00} = 1 - V_{0000}^{Coul}\pi_{00}^{(0)}$) is calculated using the plasmon pole approximation. This technique was first introduced as a simplified means of treating electron correlations in metals,[10] but has, more recently, been applied[2,6] to inversion layers on the surface of silicon. In principle, the plasmon pole treatment is an approximation to the RPA. In practice, it greatly simplifies the self-energy calculation by replacing an integral expression for $\pi_{00}^{(0)}$ (which must, in general, be evaluated numerically) with an analytic form.

Combining Eq. (24) for the self-energy with a dressed interaction of the form (26) yields

$$\hbar M_{00}(\vec{k}, \omega) = \hbar M_{00}^{Coul}(\vec{k}, \omega) + \hbar M_{00}^{ph}_{0000}(\vec{k}, \omega) + \hbar M_{11}^{ph}_{1010}(\vec{k}, \omega),$$

$$(28)$$

$$\hbar M_{11}(\vec{k}, \omega) = \hbar M_{11}^{Coul}_{1111}(\vec{k}, \omega) + \hbar M_{11}^{ph}(\vec{k}, \omega) + \hbar M_{00}^{ph}_{1010}(\vec{k}, \omega),$$

$$(29)$$

$$\hbar M_{10}(\vec{k}, \omega) = \hbar M_{01}(\vec{k}, \omega) \quad (30)$$

$$= \hbar M_{00}^{ph}_{0001}(\vec{k}, \omega) + \hbar M_{11}^{ph}_{0111}(\vec{k}, \omega), \quad (31)$$

where

$$\hbar M_{nn}^{Coul}(\vec{k}, \omega) = (i)\frac{A}{(2\pi)^3}$$

$$\times \int d^2\vec{q}\, d\omega' U_{nnnn}^{Coul}(\vec{q}, \omega')$$

$$\times G_{nn}^{0}(\vec{k}-\vec{q}, \omega-\omega')e^{i\omega'\eta} \quad (32)$$

and

$$\hbar M_{nn}^{ph}_{ijlm} = (i)\frac{A}{(2\pi)^3}$$

$$\times \int d^2\vec{q}\, d\omega' V_{ijlm}^{e-ph}(\vec{q}, \omega')$$

$$\times G_{mm}^{0}(\vec{k}-\vec{q}, \omega-\omega')e^{i\omega'\eta}. \quad (33)$$

It has been assumed that only the two lowest subbands ($n = 0$ and $n = 1$) are important and that the infinite self-energy matrix may be adequately approximated using a (2 × 2) form. As will be shown, this assumption, while apparently rather drastic, is justified by the results obtained.
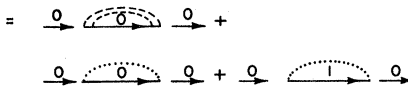
Figures 1(a), 1(b), and 1(c) are diagrammatic representations of the matrix elements M_{00}, M_{11}, and M_{10}, respectively. Notice that, in addition to the appearance of the nonzero off-diagonal elements (M_{10} and M_{01}), the present approach results in the appearance of additional terms $M_{nn}^{ph}_{1010}$, which contribute to the *diagonal* self-energy but have no analog in the diagonal approximation.

The approximate form for the self-energy, Eqs. (28)–(31), can be combined with Eqs. (19) and (23) and solved self-consistently to obtain the quasiparticle excitation energies [self-consistently because $\vec{M}(\vec{k}, E_i(k))$ is, itself a function of the quasiparticle energy]. Here, however, this method has not been used. Rather, the self-energy matrix is calculated using the Hartree energy $\epsilon_i(k)$, and the quasiparticle energies $E_i(k)$, determined as the solution of the simpler equation
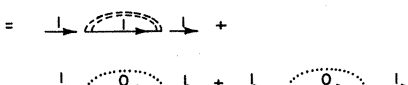
$$\left|[G^0(k, E_i(k))]^{-1} - M(\vec{k}, \epsilon_i(\vec{k}))\right| = 0. \quad (34)$$

In addition to being a simplification of considerable

(a) $M_{00}(k,\omega) = M_{00}^{Coul}(k,\omega) + M_{00}^{ph}_{0000}(k,\omega) + M_{11}^{ph}_{1010}(k,\omega)$

(b) $M_{11}(k,\omega) = M_{11}^{Coul}_{1111}(k,\omega) + M_{11}^{ph}(k,\omega) + M_{00}^{ph}_{1010}(k,\omega)$

(c) $M_{10}(k,\omega) = M_{01}(k,\omega)$

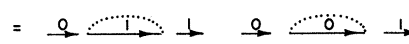$$= M_{00}^{ph}_{0001}(k,\omega) + M_{11}^{ph}_{0111}(k,\omega)$$

FIG. 1. (a) Feynman diagrams included in the calculation of the ground subband self-energy. (b) Feynman diagrams included in the calculation of the self-energy of the first excited subband. (c) Feynman diagrams included in the calculation of the nondiagonal elements of the self-energy matrix.

practical importance, the approximation is also believed[11] to be more consistent with our use of low-order corrections to the effective interaction.

B. Results and conclusions

Figure 2 is a plot of the self-energy as a function of subband index ($n = 0$ and $n = 1$) and wave vector (k/k_F where k_F is the Fermi wave vector) at an inversion-layer density of $N_{inv} = 7 \times 10^{11}$ cm^{-2}. The input data, shown in Table I, correspond to a GaAs substrate with a relatively low acceptor doping ($N_A - N_D) = 1 \times 10^{15}$ cm^{-3}, or $N_{depl} = 1.44 \times 10^{11}$ cm^{-2}. The insulator dielectric constant ϵ_i corresponds to that of a native oxide[12] grown on GaAs. The actual value of this quantity varies somewhat with composition and fabrication technique, but the value used is typical of insulators currently produced.

In Fig. 2, the Coulomb self-energy (dashed line designated Coulomb) calculated in the diagonal RPA is compared to the self-energy obtained when diagonal and nondiagonal phonon effects are included (solid line designated phonon). It should be remembered that the phonon self-energy plotted is *not*, as in our earlier calculation, the value of a (single) self-energy integral. Rather, it is the difference between the Hartree energy and the total quasiparticle energy obtained by solving Eq. (34):

$$\bar{M}_{ii}(\vec{k}, \epsilon_i(\vec{k})) = E_i(\vec{k}) - \epsilon_i(\vec{k}) . \qquad (35)$$

(The "bar" indicates that the quantity has been obtained by diagonalizing the Green's-function matrix.) This quantity differs, in principle, from the quantities M_{ii} obtained in Eqs. (28) and (29); the latter represent the self-energy in the absence of intersubband mixing.
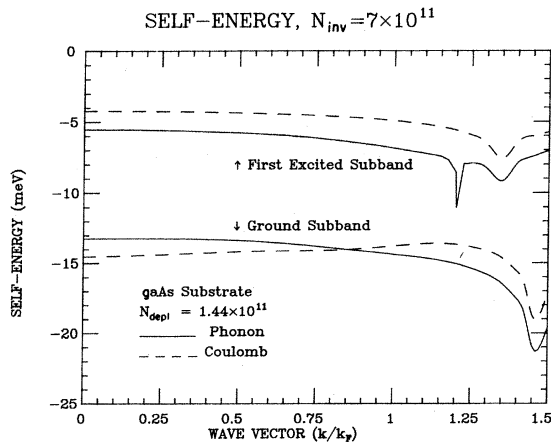
However, in all cases checked, *including* values of N_{inv} such that the subband separation is nearly equal to the LO-phonon energy, it is found that

$$\bar{M}_{ii}(\vec{k}, \epsilon_i(\vec{k})) = M_{ii}(\vec{k}, \epsilon_i(\vec{k})) \qquad (36)$$

within the estimated numerical accuracy of the calculation (typically better than 1%). That is, the intersubband mixing of states due to the phonon-mediated interaction is completely negligible. The result confirms the validity of our earlier diagonal calculation and also justifies use of the two-subband model.

The current results agree qualitatively with those obtained using the diagonal approximation (see discussion in Ref. 1). Here, however, positive phonon contributions to the self-energy appear more dominant than they were in the earlier calculation where such terms were negative except at the highest density ($N_{inv} = 1 \times 10^{12}$ cm^{-2}) and at small wave vector. Here, the phonon self-energies are positive at densities as low as 4×10^{11} cm^{-2} and at relatively larger wave vector.

Notice that a very sharp dip occurs in the self-energy of the first excited subband at $k/k_F \approx 1.2$. A similar structure is found at other inversion-layer densities, and always occurs at a value of $|k|$ such that

$$\hbar^2 k^2 / 2m^* = \hbar \omega_{LO} . \qquad (37)$$

That is, it occurs when $\epsilon_1(\vec{k})$ is just large enough to allow the state to decay by emission of an LO phonon. The peak may be attributed to *intrasubband* mixing of states and is extremely narrow because no phonon damping or dispersion has been included in the theory. A reexamination of the results of our earlier diagonal calculation[1] indicates that the structure is also present in that theory, but was not evident because of its sharpness.

Also notice that broad, deep dips appear in the self-energy of the ground ($k/k_F \approx 1.45$) and first excited ($k/k_F \approx 1.35$) subbands. Since the structure appear in both the diagonal Coulomb and phonon approximations, they can, again, be attributed to the *intrasubband* mixing of states. The dip in the ground subband has been identified with states whose (Hartree) energy is just far enough above the Fermi energy to allow decay by emission of an *effective* 2D plasmon, $\bar{\omega}_p(\vec{q})$. However, $\bar{\omega}_p$ is *not* a real plasmon, but rather an artifact of the plasmon pole approximation.[2,6] Since in this approximation all the absorption strength of the system is assumed to be concentrated in a single "plasmon pole" at $\bar{\omega}_p$, its appearance inside the single-particle continuum indicates that the theory may not be valid when $\epsilon_0(\vec{k}) \gtrsim \hbar \bar{\omega}_p(\vec{k})$ (the theory, however, remains valid for lower energies and

SELF—ENERGY, $N_{inv} = 7 \times 10^{11}$

↑ First Excited Subband

↓ Ground Subband

gaAs Substrate
$N_{depl} = 1.44 \times 10^{11}$

——— Phonon
– – – – Coulomb

FIG. 2. Self-energy as a function of subband index and wave vector for an inversion-layer density of 7×10^{11} cm^{-2}. The Coulomb and phonon (phonon plus Coulomb) approximations have been compared.

TABLE I. Parameters valid for a GaAs substrate.

High-frequency dielectric constant	$\epsilon_\infty = 10.48$
Static dielectric constant	$\epsilon_\infty = 12.35$
Insulator dielectric constant	$\epsilon_i = 3.75$
Phonon frequency	$\hbar\omega_{LO} = 36.8$ meV
Band effective mass	$m^* = 0.0658 m_e$
Acceptor excess	$N_A - N_D = 1.0 \times 10^{15}$ cm^{-3}
Depletion layer density	$N_{depl} = 1.44 \times 10^{11}$ cm^{-2}

also for higher subbands because of the weak intersubband coupling). The dip in the first excited subband has not been identified.

Figure 3 is a plot, valid for GaAs inversion layers, of the subband separation E_{10} as a function of density. The difference in quasiparticle energies is calculated in the limit that $k \to 0$. That is

$$E_{10} = \lim_{\vec{k} \to 0} [E_1(\vec{k}) - E_0(\vec{k})] . \qquad (38)$$

The results have been calculated in the two-subband phonon approximation, the diagonal Coulomb approximation, and the Hartree approximation. As in our earlier diagonal calculation, the two many-particle theories yield similar results. However, the current unscreened phonon approximation does predict slightly smaller subband separations than the diagonal screened phonon approximation. As before, the Hartree approximation yields a considerably different result and, thus, reemphasizes the importance of many-particle effects in low-band-mass semiconductors.

In Fig. 4 the subband separation has been calcu-

lated as a function of density for inversion layers on the surface of InP. The relevant input data are shown in Table II, and correspond to a substrate doping $(N_A - N_D = 1 \times 10^{16}$ cm$^{-3})$, or to a depletion layer concentration of $N_{depl} = 4.32 \times 10^{11}$ cm^{-2}. The insulator is assumed to be deposited SiO$_2$ [currently the most promising insulator for the construction of metal-insulator-semiconductor (MIS) structures on this semiconductor]. As for GaAs the results of the two-subband phonon, the diagonal Coulomb, and the Hartree approximations have been compared.

The results obtained for the subband separation (and also the self-energy) of inversion layers on InP are similar to those obtained on the surface of GaAs. However, the subband separation in this case tends to be somewhat greater due, principally, to the larger depletion-layer density and the resulting stronger surface electric field. In addition, the phonon contribution is somewhat more significant than it is on GaAs. The result is reasonable since InP is a more polar material
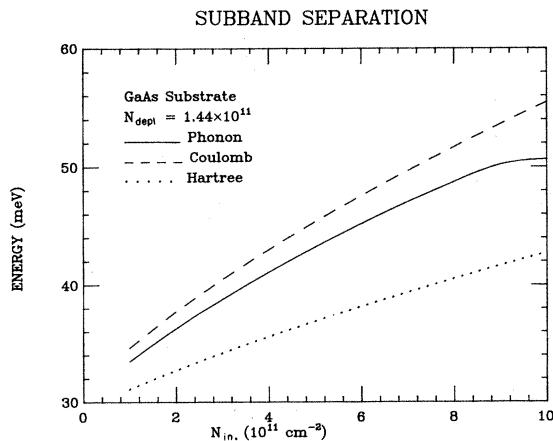
SUBBAND SEPARATION

FIG. 3. Subband separation (E_{10}) of GaAs inversion layers as a function of density. The results of a Coulomb and phonon calculation are compared to the results of the Hartree approximation.
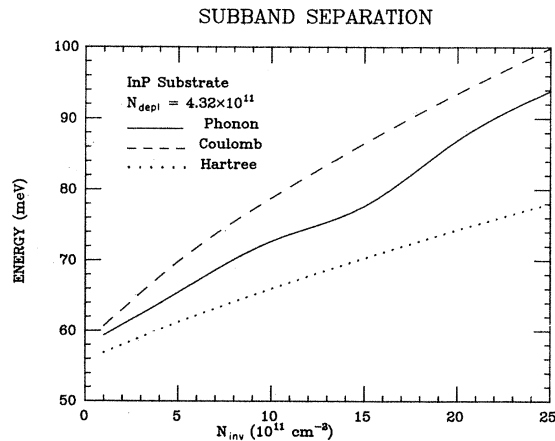
SUBBAND SEPARATION

FIG. 4. Subband separation (E_{10}) of InP inversion layers as a function of density. The results of a Coulomb and phonon calculation are compared to the results of the Hartree approximation.

TABLE II. Parameters valid for an InP substrate.

High-frequency dielectric constant	$\epsilon_\infty = 9.6$
Static dielectric constant	$\epsilon_0 = 12.6$
Insulator dielectric constant	$\epsilon_i = 3.9$
Phonon frequency	$\hbar\omega_{LO} = 42.8$ meV
Band effective mass	$m^* = 0.0803 m_e$
Acceptor excess	$N_A - N_D = 1.0 \times 10^{16}$ cm^{-3}
Depletion layer density	$N_{depl} = 4.32 \times 10^{11}$ cm^{-2}

than GaAs (i.e., ϵ_0 and ϵ_∞ differ by a larger amount).

IV. DEPOLARIZATION

A. Theory

The depolarization or resonant screening effect is an experimental artifact which is observed when subband structure is examined using far-infrared (FIR) absorption techniques. In silicon inversion layers, depolarization merely shifts the observed absorption peak to energies larger than the subband separation E_{10}. In polar semiconductors, however, the presence of a frequency-resonant interaction splits the observed absorption peak into two branches which have interpretation as mixed electron-phonon excitations.

The effect was first discussed in connection with a similar problem in the thin films.[13] Calculations dealing specifically with inversion layers on silicon (100) surfaces have been carried out by Allen et al.,[3] Nakayama,[14] and Vinter.[2] These authors point out that the absorption occurs at the poles of the conductivity tensor

$$\sigma_{zz}(\vec{k} \to 0, \omega) \to \infty, \tag{39}$$

where, in general, we may restrict our attention to the z component of the applied electric field and to vertical ($\vec{k} \to 0$) optical transitions.

The present calculation utilizes a many-particle approach[15] to find the linear response of the inversion layer to an applied electric field.[16] The power absorbed is obtained as a function of the conductivity, and the position of the absorption peaks is determined by finding the poles of $\sigma_{zz}(\vec{k} \to 0, \omega)$. The calculation loosely follows the treatment outlined by Vinter[2] for silicon inversion layers. Our derivation, however, includes the frequency-dependent electron-phonon interaction and also provides a means for calculating the relative absorption strength as a function of density.

It is convenient to use Fourier transforms in the x-y plane and in time (but not, as in earlier sections, in the z direction). Then, a straightforward

linear-response calculation[16] can be used to derive the density fluctuation, $\delta \langle n(\vec{k}, \omega; z) \rangle$, due to an applied external potential $[\phi(\vec{k}, \omega; z)]$ as

$$\delta \langle n(\vec{k}, \omega; z) \rangle = -e \int_0^\infty dz'' \pi^R(\vec{k}, \omega; z, z'') \phi(\vec{k}, \omega; z''), \tag{40}$$

where $\pi^R(\vec{k}, \omega; z, z'')$ is the transform of the retarded density-density correlation function (and will be discussed in more detail later). Using the continuity equation

$$\frac{\partial}{\partial z}[j_z(\vec{k}, \omega; z)] = (i\omega)e^2 \int_0^\infty dz'' \pi^R(\vec{k}, \omega; z, z'')$$
$$\times \phi(\vec{k}, \omega; z''), \tag{41}$$

and integrating with respect to z,

$$j_z(\vec{k}, \omega; z) = (i\omega)e^2 \int_0^z dz' \int_0^\infty dz'' \pi^R(\vec{k}, \omega; z', z'')$$
$$\times \phi(k, \omega; z''). \tag{42}$$

Now assume that

$$\phi(\vec{k}, \omega; z'') = z'' E_z(\vec{k}, \omega). \tag{43}$$

This is the usual "dipole" approximation and is valid if the wavelength of the exciting radiation is much larger than the average width of the inversion layer. The approximation is well justified for the inversion-layer system and the linear current response becomes

$$j_z(\vec{k}, \omega; z) = \left((i\omega)e^2 \int_0^z dz' \int_0^\infty dz'' z'' \pi^R(\vec{k}, \omega; z', z'')\right)$$
$$\times E_z(\vec{k}, \omega). \tag{44}$$

Finally, the total power absorbed per unit area (due to currents in the z direction) is

$$P(\vec{k}, \omega) = \tfrac{1}{2}\,\text{Re} \int_0^\infty dz\, j_z(\vec{k}, \omega; z) E_z(\vec{k}, \omega) \tag{45}$$

$$= \tfrac{1}{2}\,\text{Re}\, \sigma_{zz}(\vec{k}, \omega) |E_z(\vec{k}, \omega)|^2, \tag{46}$$

where

$$\sigma_{zz}(\vec{k}, \omega) = (i\omega)e^2 \int_0^\infty dz \int_0^z dz' \int_0^\infty dz'' z''$$

$$\times \pi^R(k, \omega; z', z'') . \quad (47)$$

The quantity $\sigma_{zz}(\vec{k}, \omega)$ is the (z, z) component of an _effective_ conductivity tensor. It is, however, _not_ a true conductivity in the normal sense because it is not directly related to a current response. Rather σ_{zz} is an average of the current response over all z and is related to the total power absorbed per unit area (per unit frequency) in the same way that a true conductivity tensor would be

related to the power absorbed per unit volume. However, it is the poles of $\mathrm{Re}(\sigma_{zz})$ in the limit $k \to 0$, which define the positions of the absorption peaks in an optical absorption experiment. In addition the strength of these poles is proportional to the strength of the absorption, a result which provides a convenient means of calculating the relative absorption strength as a function of inversion-layer density.

The (retarded) quantity, $\pi^R(\vec{k}, \omega; z', z'')$, appearing in the definition of σ_{zz} [Eq. (47)] may be expanded in terms of ξ_i. Restricting attention to the limit $k \to 0$, and assuming that the Green's function is diagonal,

$$\pi^R(k \to 0, \omega; z', z'') = \sum_{i,j} [\xi_i(z')\xi_j(z')][\xi_j(z'')\xi_i(z'')]\pi_{ij}(k \to 0, \omega + i\eta) . \quad (48)$$

Here, the retarded polarizability has been found from its time-ordered form by replacing $\omega \to \lim_{\eta \to 0}$ $(\omega + i\eta)$. The form is correct for the real ξ_i introduced in Sec. II. In the special case that only the ground subband is occupied, Vinter[2] finds

$$\pi_{ij}(k \to 0, \omega) \approx \begin{cases} \pi_{i0}^{(0)}(k \to 0, \omega) = -\dfrac{N_{\mathrm{inv}}}{(\hbar\omega) + E_{i0}}, & i \neq 0, j = 0 \\[2ex] \pi_{0j}^{(0)}(k \to 0, \omega) = \dfrac{N_{\mathrm{inv}}}{(\hbar\omega) - E_{j0}}, & i = 0, j \neq 0 \\[2ex] 0 \quad \text{otherwise.} \end{cases} \quad (49)$$

Combining Eqs. (47), (48), and (49) and ignoring all but the first two subbands yields

$$\sigma_{zz}(k \to 0, \omega) = (i\omega)e^2 |z_{10}|^2 \chi_{10}^{(0)}(k \to 0, \omega + i\eta) , \quad (50)$$

where z_{ij} is a dipole matrix element defined (for real ξ_i) by

$$z_{ij} = \int_0^\infty dz \, \xi_i(z) z \xi_j(z) \quad (51)$$

and

$$\chi_{ij}^{(0)}(\vec{k}, \omega) = \pi_{ij}^{(0)}(\vec{k}, \omega) + \pi_{ji}^{(0)}(\vec{k}, \omega) . \quad (52)$$

The quantity $\chi_{ij}^{(0)}$ is shown schematically in Fig. 5(a); it represents the lowest-order approximation to χ_{ij} and yields the particularly simple (though incorrect) result that absorption occurs at the subband separation, E_{10}.

In a simple extension of this theory which includes depolarization, $\chi_{ij}^{(0)}(\vec{k}, \omega)$ is replaced by $\chi_{ij}^{(1)}(\vec{k}, \omega)$ defined, as shown in Fig. 5(b), by Dyson's equation

$$\chi_{10}^{(1)}(\vec{k} \to 0, \omega + i\eta) = \frac{\chi_{10}^{(0)}(k \to 0, \omega + i\eta)}{1 - V_{1010}^{e-e}(\vec{k} \to 0, \omega + i\eta) \chi_{10}^{(0)}(k \to 0, \omega + i\eta)} . \quad (53)$$

Replacing $\chi_{10}^{(0)}$ by $\chi_{10}^{(1)}$ in Eq. (50) and using the identity

$$\lim_{\eta \to 0} \frac{1}{\omega \pm i\eta} = P\left(\frac{1}{\omega}\right) \mp i\pi\delta(\omega) \quad (54)$$

yields

$$\mathrm{Re}\,\sigma_{zz}(k \to 0, \omega) = -\left(\frac{\pi e^2}{\hbar^2}\right)(N_{\mathrm{inv}} E_{10}) \, (|Z_{10}|^2) \frac{\omega^2 - \omega_{\mathrm{LO}}^2}{\Omega_+^2 - \Omega_-^2}$$

$$\times \left(\frac{\omega}{\Omega_+}[\delta(\omega - \Omega_+) - \delta(\omega + \Omega_+)] - \frac{\omega}{\Omega_-}[\delta(\omega - \Omega_-) - \delta(\omega + \Omega_-)]\right), \quad (55)$$

where

$$\Omega_\pm^2 = \tfrac{1}{2}(\omega_{10}^2 + \omega_{LO}^2 + \Omega^2) \pm \tfrac{1}{2}\{(\omega_{10}^2 + \omega_{LO}^2 + \Omega^2)^2 - 4[\omega_{10}^2 + (1-\alpha)\Omega^2]\omega_{LO}^2\}^{1/2},$$ (56)

$$\Omega^2 = \left(\frac{2N_{inv}E_{10}}{\hbar^2}\right)\left(\frac{4\pi e^2}{\epsilon_\infty}S_{11}\right),$$ (57)

$$\alpha = 1 - \frac{\epsilon_\infty}{\epsilon_0},$$ (58)

$$S_{11} = \int_0^\infty dz\left(\int_0^z dz'\xi_0(z')\xi_1(z')\right)^2.$$ (59)

Equation (55) shows immediately that the poles of $\sigma_{zz}(k \to 0, \omega)$ occur at two distinct frequencies, Ω_+ and Ω_-; the single electronic excitation is observed as *two* peaks in the absorption spectrum. An examination of Eq. (56) shows that

$$\Omega_+ \geq \omega_{10} = \frac{1}{\hbar}E_{10}$$ (60)

and

$$\Omega_- \leq \omega_{LO}.$$ (61)

These results indicate that the depolarization splitting cannot be responsible for the observed

(a) $\quad \chi_{10}^{(0)}(q \to 0,\omega) =$

(b) $\quad \chi_{10}^{(1)}(q \to 0,\omega) = \chi_{10}^{(0)}(q \to 0,\omega)$

$\qquad + \chi_{10}^{(0)}(q \to 0,\omega)\, V_{1010}^{e\text{-}e}(q \to 0,\omega)\, \chi_{10}^{(1)}(q \to 0,\omega)$
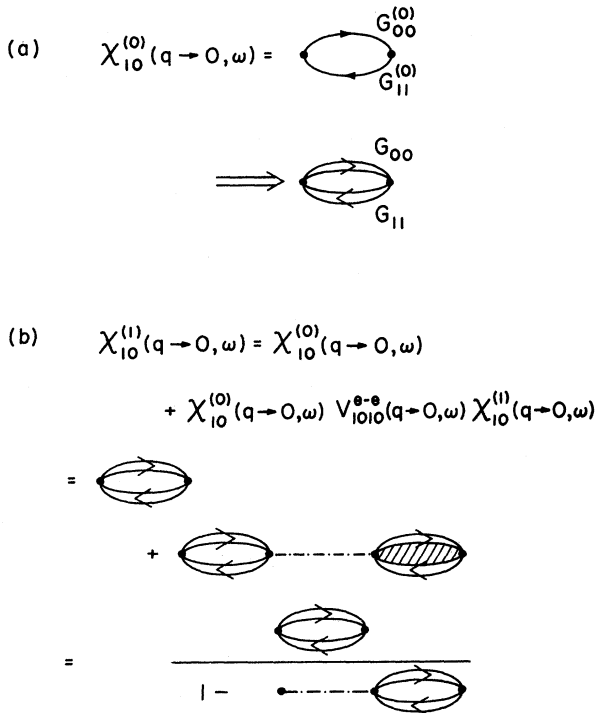
FIG. 5. Feynman diagrams representing the intersubband polarizability in (a) the lowest-order approximation, and (b) the first-order approximation which includes depolarization effects.

"double" peak in InSb inversion layers. In such experiments all absorption peaks were observed at energies greater than $\hbar\omega_{LO}$. The depolarization phenomenon discussed here has not yet been observed in inversion layers.

As already mentioned Ω_+ and Ω_- are the excitation energies of mixed electron-phonon states. An examination of $\Omega_\pm$ indicates that, at large subband separation ($E_{10} > \hbar\omega_{LO}$ or N_{inv} large; valid for most obtainable densities), the upper branch (Ω_+) is "electronlike" and the lower branch (Ω_-) is "phononlike." That is, the electronlike Ω_+ branch behaves as a simple (as in silicon inversion layers) depolarization-shifted electronic excitation, and the lower phononlike branch behaves as a nearly dispersionless phonon excitation. At the very low (and less important) densities, however, the roles are reversed.

The strength of the poles of σ_{zz} can also be obtained directly from Eq. (55). That strength is

$$-\left(\frac{\pi e^2}{\hbar^2}\right)(N_{inv}E_{10})(|z_{10}|^2)\left.\frac{(\omega^2 - \omega_{LO}^2)}{(\Omega_+^2 - \Omega_-^2)}\right|_{\omega=\Omega_\pm}.$$ (62)

This quantity is proportional to the size of (i.e., area under) the absorption peak. Notice that the strength is calculated in terms of the dipole matrix element $|z_{10}|$ and the form factor S_{11}. Since these quantities [defined in Eqs. (51) and (59), respectively] depend on the envelope functions ξ_i, a measurement of absorption amplitude can be used to obtain information concerning the wave functions themselves.

B. Results and conclusions

Figure 6 is a plot of the two absorption frequencies, Ω_+ and Ω_-, as a function of N_{inv} for a GaAs substrate. Other parameters are listed in Table I. For comparison, the dashed line shows the subband separation calculated using the two-subband approximation, and the dotted line is the LO-phonon energy.

It is evident that the upper electronlike branch is shifted to higher energies relative to the subband separation. While the shift is quite large (20–30%), actual observation of the upper absorption branch may, in fact, occur at somewhat lower
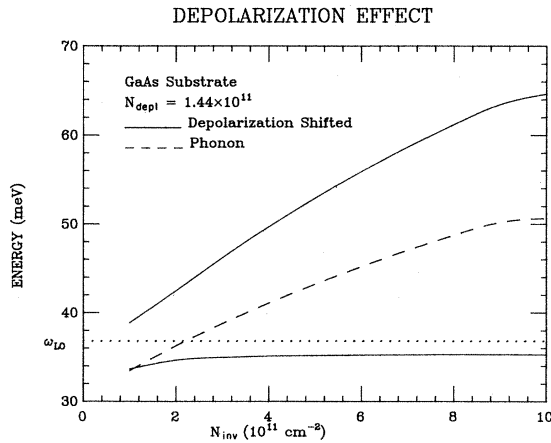
DEPOLARIZATION EFFECT

FIG. 6. Upper and lower depolarization-shifted absorption branches for GaAs inversion layers. The subband separations (calculated in the phonon approximation) is shown as a dashed (-----) line, and LO-phonon energy is shown as a dotted (·····) line.

DEPOLARIZATION EFFECT

FIG. 8. Upper and lower depolarization-shifted branches for InP inversion layers.

energy due to the excitonic shift.[2,17] The latter effect has not been included in the present calculation, but accounts for the interaction between the excited electron and its remaining hole. Calculations valid for silicon inversion layers and including this effect show that the excitonic shift tends to cancel depolarization effects and results in an observed absorption peak which is somewhat closer to the calculated subband separation. While such calculations, valid for GaAs inversion layers, have not yet been performed, it is probable that a similar cancellation between depolarization and excitonic effects will be found.

The lower branch is phononlike over most of the density range and appears about 1 meV below the bulk phonon energy. While this absorption peak

corresponds to the creation of a (mostly) lattice vibration, it is *not* associated with the direct excitation of a bulk LO phonon. Instead, the excitation is created through an indirect, inversion-layer-mediated coupling between the lattice and the external radiation field.

The relative strength of the absorption as a function of density (N_{inv}) is shown in Fig. 7. The upper (solid) curve is valid for the upper, electronlike branch and the lower (dashed) curve is valid for the lower, phononlike branch. Other parameters are shown in Table I. Notice that the curves cross at a very low inversion-layer density. The crossing suggests a change in the electron- and/or phonon-like character of the branches.

Figures 8 and 9 are plots of the depolarization shift and absorption amplitude as a function of inversion-layer density for an InP substrate. The
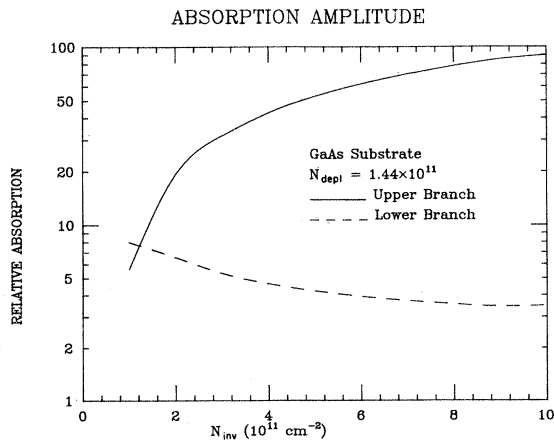
ABSORPTION AMPLITUDE

FIG. 7. Relative absorption amplitudes of the upper and lower depolarization-shifted branches as a function of inversion-layer density. The substrate is GaAs.
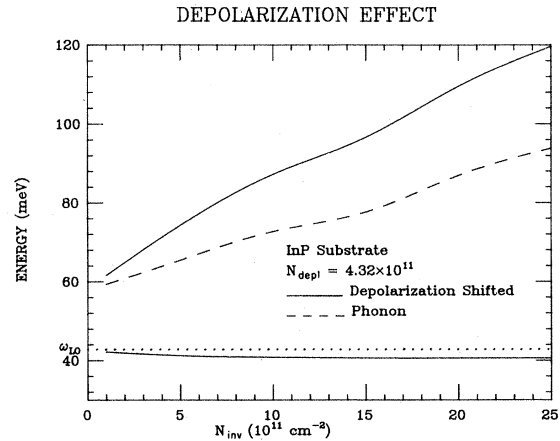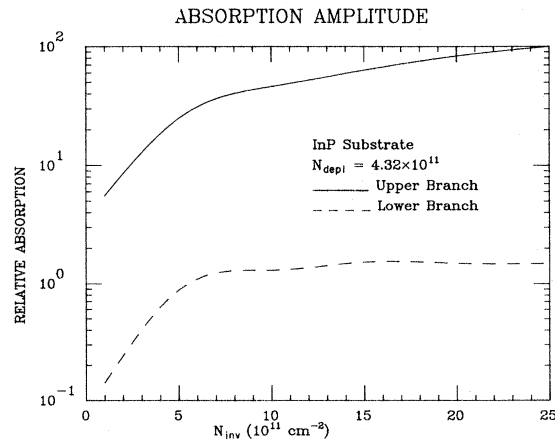
ABSORPTION AMPLITUDE

FIG. 9. Relative absorption amplitudes of the upper and lower depolarization-shifted branches as a function of inversion-layer density. The substrate is InP.

other parameters are shown in Table II. Again, the results are very similar to those obtained for GaAs inversion layers. Here, however, the subband separation is larger and results in an upper branch which is distinctly electronlike and a lower branch which is distinctly phononlike for all densities examined.

V. SUMMARY

In this paper, we have calculated the self-energy and quasiparticle energy of inversion-layer electrons on the surface of polar semiconductors. As in our earlier diagonal calculation, the Coulomb and LO-phonon—mediated interactions between electrons have been included in a many-particle calculation for the self-energy. However, the model used here treated an unscreened electron-phonon interaction, but did include the effects of subband mixing due to this term. A simple two-subband model was used to calculate the quasiparticle energy. This particularly simple model indicated that the subband mixing is quite negligible even when the subband separation is very close

to the LO-phonon frequency.

The quasiparticle energies obtained were also used as the basis for a depolarization calculation including the frequency—resonant-LO-phonon interaction. It was found that FIR absorption experiments should detect two absorption peaks associated with each intersubband transition. The lower branch is phononlike and very weak for most inversion-layer densities. However, in very pure samples of GaAs or InP and at relatively small electron density (i.e., when $E_{10} \lesssim \hbar\omega_{LO}$) the lower branch becomes stronger and more electronlike. Under these conditions, it may be more readily observable and could prove to be an interesting means of probing the inversion-layer system itself.

ACKNOWLEDGMENT

[1]G. H. Kawamoto, R. Kalia, J. J. Quinn, Proceedings of the Third International Conference (Yamada Conference III on the Electronic Properties of 2D Systems, Yamada, 1979 [Surf. Sci. (in press)].
[2]B. Vinter, Phys. Rev. B 15, 3947 (1977).
[3]S. J. Allen, D. C. Tsui, and B. Vinter, Solid State Commun. 20, 425 (1976).
[4]K. Weisinger, W. Beinvogl, and F. Koch, Proceedings of the Fourteenth International Conference on the Physics of Semiconductors, Edinburgh, 1978, edited by B. L. H. Wilson (The Institute of Physics, Bristol, 1978), p. 1215.
[5]W. Kohn, in Advances in Solid State Physics edited by F. Seitz, D. Turnbull, and H. Ehrenreich (Academic, New York, 1957), Vol. 5.
[6]S. DasSarma, R. K. Kalia, M. Nakayama, and J. J. Quinn, Phys. Rev. B 19, 6397 (1979).
[7]T. K. Lee, C. S. Ting, and J. J. Quinn, Solid State Commun. 16, 1309 (1975).
[8]R. Evard, in Polarons in Ionic Crystals and Polar Semiconductors, Scottish Universities Summer School, edited by Jozef T. Devreese (North-Holland, Amsterdam, 1972).
[9]G. D. Mahan, in Polarons in Ionic Crystals and Polar Semiconductors, Scottish Universities Summer School, edited by Jozef T. Devreese (North-Holland, Amsterdam, 1972).
[10]A. W. Overhauser, Phys. Rev. B 3, 1888 (1971).
[11]T. M. Rice, Ann. Phys. (N.Y.) 31, 100 (1965).
[12]R. P. H. Chang and J. J. Coleman, Appl. Phys. Lett. 32, 332 (1978).
[13]W. P. Chen, Y. S. Chen, and E. Burstein, Surf. Sci. 58, 263 (1976).
[14]M. Nakayama, Solid State Commun. 21, 587 (1977).
[15]A. L. Fetter and J. D. Walecka, Quantum Theory of Many-Particle Systems (McGraw-Hill, New York, 1971).
[16]D. A. Dahl and L. J. Sham, Phys. Rev. B 16, 651 (1977).
[17]T. Ando, Phys. Rev. B 13, 3468 (1976).